

A Combined Pathway to Simulate CDK-dependent phosphorylation and ARF-dependent Stabilization for p53 Transcriptional Activity

Atsushi Doi¹

doi@ims.u-tokyo.ac.jp

Masao Nagasaki¹

masao@ims.u-tokyo.ac.jp

Kazuko Ueno¹

uepi@ims.u-tokyo.ac.jp

Hiroshi Matsuno²

matsuno@sci.yamaguchi-u.ac.jp

Satoru Miyano¹

miyano@ims.u-tokyo.ac.jp

¹ Human Genome Center, Institute of Medical Science, University of Tokyo, 4-6-1 Shirokanedai, Minato-ku, Tokyo 108-8639, Japan

² Graduate School of Science and Engineering, Yamaguchi University, 1677-1 Yoshida, Yamaguchi, 753-8512, Japan

Abstract

The protein p53 is phosphorylated by a member of protein kinases such as CDK7, and stabilized by the protein ARF. The phosphorylation and stabilization of p53 is believed to enhance its transcriptional activity and act simultaneously. Biological pathways composed of experts knowledge obtained from the literature are including these activation mechanisms. However, the map of biological pathways does not reflect the combination effect of phosphorylation and stabilization.

We have conducted some simulations of biological pathways with hybrid functional Petri net (HFPN) after careful reading of papers. In this paper, we constructed the HFPN based biological pathway of CDK-dependent phosphorylation pathway and combine with ARF-dependent pathway described previously, to observe the effect of the phosphorylation on the stabilization with simulation-based validation.

Keywords: biological pathway, Petri net, simulation, p53, transcriptional activity

1 Introduction

Biological processes are usually summarized in a picture composed of figures of various shapes (e.g. circles and rectangles) and several types of arrows. Graphical images in the picture are important since they reflect the knowledge in biology and medicine. The summarized picture make a network called “Biological Pathway”.

Biological pathway databases such as BioCyc [1], KEGG [13, 2], and TRANSPATH [15, 3] have compiled many biological processes between cellular components, providing invaluable information to researchers in the forms of pictures. However, with such databases, it is not easy to grasp the information about quantitative interactions of molecules, since such databases focus on providing qualitative information of biological processes.

We have conducted some simulations of biological pathways with hybrid functional Petri net (HFPN) [9, 11, 20]. HFPN have been introduced Matsuno et al. [18] and is a representation method for biological pathways.

A gene *p53* is called a tumor suppressor gene since *p53* regulate cell cycle arrest and induces apoptosis. A modification of the protein p53 complicates the relationship between the concentration of p53 and its transcriptional activity. The protein p53 is stabilized by the protein ARF [22] and phosphorylated by kinases [14, 28, 22, 16, 7, 26, 27, 8, 25]. The pathway databases store these information of stabilization and phosphorylation in a map. Although the map describes molecular

interactions between the proteins p53, ARF and kinases, the synegetic effect of the stabilization and the phosphorylation is still unclear.

We have constructed the ARF-dependent stabilization pathway and attempted the simulation-based validation of the p53 transcriptional activity with hybrid functional Petri net [11]. In this paper, we represent the CDK-dependent phosphorylation pathway with HFPN and combine this phosphorylation pathway with ARF-dependent stabilization pathway [11]. We demonstrated the effect which was not observed in the single, combining two pathways by the simulation-based validation.

2 Biological Pathway Representation with Hybrid Functional Petri Net

A Petri net, defined by Carl Adam Petri, is a mathematical method which has visual expression like a pathway and allows us to describe the dynamics of systems [23]. It has been mainly used so far to model artificial systems such as manufacturing systems and communication protocols. A Petri net is a network consisting of “places”, “transitions”, “arcs” and “tokens”. Places are represented by a circle which can hold the tokens. Transitions are represented by a rectangle, having a function of transmitting the tokens from the places. Arcs have a direction and connect a place (transition) and a transition (place).

Biological processes include the information of concentrations of substances such as proteins and mRNAs. Their value is a continuous value. Because of that, to express biological processes, we need the expression which can handle continuous value. However, the information that “a protein is activated or not” is included as the biological processes, which can be expressed by discrete event. Hence, we need expressions which can handle discrete value. To handle both of the continuous and discrete information, we employed the hybrid Petri net (HPN) [6] for modeling and simulating a biological pathway [19]. Moreover we have defined hybrid functional Petri net (HFPN) [20] as an extension of the HPN and developed a software Cell Illustrator for modeling and simulation of biological pathways [21, 10].

We changed the symbols of “place” and “transition” to biological images on Cell Illustrator. Although these changes have no effect on mathematical meaning, it is helpful for biologists to understand the pathway. Each substance such as proteins or mRNAs corresponds to an HFPN element “place” (originally a double circle, but it is changed to a picture reflecting the biological meaning of the place: see Fig. 1), which holds the concentration of the substance.

3 CDK-dependent phosphorylation pathway with Hybrid Functional Petri Net

The protein p53 is a tumor suppressor and has a transcriptional activity. The transcriptional activity of the protein p53 depends on the concentration of the protein p53 or the phosphorylation at the N-terminal and C-terminal regions of p53. If the protein p53 is stabilized by the protein p19ARF, the concentration of p53 increases [12]. If p53 is phosphorylated by kinases, its sequence-specific DNA binding activity is enhanced [17].

Proteins p53, MDM2, and p19ARF are closely related to cancer. The protein p53 suppresses the formation of tumors, and the protein MDM2 is a negative regulator of p53. MDM2 ubiquitinates p53 and decrease the activity and stability of the protein p53. In contrast, the protein p19ARF is an inhibitor of the protein MDM2. p19ARF interacts with MDM2 and p53, and inhibits ubiquitin-mediated degradation. Thus, the ARF-dependent stabilization pathway is consisted of proteins p53, MDM2, and p19ARF. The stabilization of p53 is a quantitative alteration for transcriptional activity of p53. We have constructed the ARF-dependent stabilization pathway and attempted the simulation-based validation of the p53 transcriptional activity with hybrid functional Petri net [11]. The simulation










	Cell Illustrator (software)		
	Original symbols of HFPN		Examples of biological images
Type	Discrete	Continuous	Discrete and Continuous
Place			
Transition			
Arc	 Normal	 Test	 Inhibitory

Figure 1: Petri nets are constructed using three kind of symbols for places, transitions, and arcs. In a software Cell Illustrator, both sets of places and transitions are classified into discrete and continuous types, and places and transitions can be replaced with pictures reflecting the biological images.

results suggested that p53 should have the transcriptional activity in the trimeric complex of p53, MDM2, and p19ARF.

On the other hand, the phosphorylation of p53 is a qualitative alteration. The protein CDK7 is a kinase and interacts with proteins cycH and p36 [17].

3.1 CDK-dependent phosphorylation pathway

Fig. 2 shows an HFPN model of CDK-dependent phosphorylation pathway which has been constructed by compiling and interpreting the information of complex CDK7-cycH-p36 and the protein p53 interactions in the literature [17]. In Fig. 2, we assign the symbols of biological images to places and transitions on Cell Illustrator instead of circles and rectangles (Fig. 1). Each place is labeled with the name of the substance (e.g. p53, CDK7 mRNA). In this paper, the name of complex of two proteins A and B is represented as A_B, where places for proteins A and B are labeled with A and B. An additional name (C) or (N) is attached at the tail of a substance name, when we need to distinguish locations of substances in the cytoplasm of in the nucleus. Moreover, an additional name {p} attached at the p53 means the phosphorylated p53.

In HFPN model of this paper and [11], all places are continuous and hold a real number as its content (Table 1). Table 1 summarizes name and variable of places in Fig. 2. Initial Values which is a initial content of a place are zero. The transitions are related to p53-CDK7 interactions summarized in the second column of Table 2. Ten events (transitions T_{13}, \dots, T_{22}) have been extracted from the literature [17]. All transitions are continuous and fire at the speed of the assigned parameters in the fourth column of Table 2. The transitions d_j ($j = 1, \dots, 19$) represent natural degradation of the corresponding substances. We define the speed of natural degradation as $nX * 0.01$ (nX indicates the concentration of a corresponding substances (Table 1)).

By means of these transitions and notations for molecules, the CDK-dependent phosphorylation pathway can be described as follows: The mRNAs of the genes *p53*, *CDK7*, *cycH*, and *p36* are synthesized by the transcriptions (T_1, T_4, T_7 , and T_{10}), and translated (T_2, T_5, T_8 , and T_{11}) to the proteins (p53(C), CDK7(C), cycH(C), and p36(C)) in a cytoplasm. Then the proteins are transported (T_3, T_6, T_9 , and T_{12}) into a nucleus as transcription factors (p53(N), CDK7(N), cycH(N), and p36(N)). CDK7(N) forms the complex CDK7_cycH with cycH(N) (T_{13}). After forming the CDK7_cycH dimeric complex, CDK7_cycH forms the CDK7_cycH_p36 trimeric complex with p36 (T_{15}). p36(N) forms the complex p36_p53 with p53(N) (T_{16}). Hence, CDK7_cycH_p36 binds to p53(N) (T_{14}), More-

over, the complex CDK7_cycH binds to the complex p36_p53 (T_{17}). After forming the complex CDK7_cycH_p36_p53, the protein p53 is phosphorylated by the complex CDK7_cycH_p36 (T_{18}).

The phosphorylated p53 enhances its sequence-specific DNA binding activity [17], therefore p53{p} has a higher transcriptional activity than unphosphorylated p53 (p53(N)). The transcriptional activity of the protein p53 is represented by test arcs from the places p53(N), p53p, and p36_p53 to the transitions T_{19} , T_{20} , and T_{21} , respectively. Furthermore, the difference of the transcriptional activity between phosphorylated protein p53 and unphosphorylated protein p53 is represented by the speeds of each transition (Table 1).

Our HFPN pathway model, we manually tuned the parameters for the transitions and initial content of places so that the model is consistent the biological experiments in [17]. Thus we defined the speed of transition T_{19} is two times faster than the speed of transition T_{20} (T_{21}). The HFPN model in Fig. 2 is available from <http://genomicobject.net> including all parameters in the model and can be simulated on Cell Illustrator 2.0 [4]

Table 1: Places in the HFPN model of Fig. 2. Initial Values of all places are 0.

Places Name	Variable (nX)	Places Name	Variable (nX)
p53(N)	$n1$	p21	$n11$
p53{p}	$n2$	CDK7 mRNA	$n12$
CDK7_cycH_p36	$n3$	CDK7(C)	$n13$
CDK7(N)	$n4$	cycH mRNA	$n14$
cycH(N)	$n5$	cycH(C)	$n15$
p36(N)	$n6$	p36 mRNA	$n16$
CDK7_cycH	$n7$	p36(C)	$n17$
CDK7_cycH_p36_p53	$n8$	p53 mRNA	$n18$
p36_p53	$n9$	p53(C)	$n19$
p21 mRNA	$n10$		

3.2 The Simulation Results of CDK-dependent Phosphorylation Pathway

Fig. 3 shows the results of simulation of the CDK-dependent phosphorylation pathway (Fig. 2). Concentration behaviors of p53(N), p36_p53, p53{p}, CDK7(N), p36(N), CDK7_cycH_p36, and p21 mRNA are observed in the following combinations of two genes; *CDK7* and *p36*. We suppose that genes *p53*, *CDK7*, *cycH*, and *p36* are found in the wild type cells. We considered the following cases:

1. All genes *p53*, *CDK7*, *cycH*, and *p36* are expressed (wild type).
2. Only the transcription of the gene *CDK7* is prohibited ($CDK7^-$ single mutant; remove the transition T_7).
3. The transcriptions of genes *CDK7* and *p36* are prohibited ($CDK7^-p36^-$ double mutant; remove the transitions T_7 and T_{10}).

When all genes *p53*, *CDK7*, *cycH*, and *p36* are expressed, p21 mRNA shows is activated by phosphorylated p53 (p53p) (Fig. 3 (1)). When the transcription of the gene *CDK7* is prohibited, p21 mRNA is activated by p53 itself (p53(N)) (Fig. 3 (2)). When the transcriptions of the gene *CDK7* and *p36* are prohibited, p21 mRNA is activated by complex p36_p53 (Fig.3 (3)). Fig. 3 (1) shows that the concentration of p21 mRNA becomes higher compared to its concentration in Fig. 3 (2) and 3(3). Because we assign the faster speed for transition T_{19} than transitions T_{20} and T_{21} . Although the simulation results of CDK-dependent phosphorylation pathway are consistent with the literature [17], we could not obtain other suggestions.

Table 2: Biological facts extracted from the literature and assignments to transition in the HFPN model of Fig. 2

T_i^\dagger	biological phenomena on the literature	type of biological processes	‡	literature
T_1	Transcription of the gene <i>p53</i> .	transcription	1	–
T_2	Translation of <i>p53</i> mRNA.	translation	$n_{18} * 0.1$	–
T_3	Nuclear import of the protein p53.	nuclear import	$n_{19} * 0.1$	–
T_4	Transcription of the gene <i>CDK7</i> .	transcription	1	–
T_5	Translation of <i>CDK7</i> mRNA.	translation	$n_{12} * 0.1$	–
T_6	Nuclear import of the protein CDK7.	nuclear import	$n_{13} * 0.1$	–
T_7	Transcription of the gene <i>cycH</i> .	transcription	1	–
T_8	Translation of <i>cycH</i> mRNA.	translation	$n_{14} * 0.1$	–
T_9	Nuclear import of the protein cycH.	nuclear import	$n_{15} * 0.1$	–
T_{10}	Transcription of the gene <i>p36</i> .	transcription	1	–
T_{11}	Translation of <i>p36</i> mRNA.	translation	$n_{16} * 0.1$	–
T_{12}	Nuclear import of the protein p36.	nuclear import	$n_{17} * 0.1$	–
T_{13}	The protein CDK7 binds to cycH.	binding	$n_4 * n_5 * 0.01$	[17]
T_{14}	The protein p53 binds to complex CDK7_cycH_p36.	binding	$n_1 * n_3 * 0.01$	[17]
T_{15}	The protein p36 binds to complex CDK7_cycH.	binding	$n_6 * n_7 * 0.01$	[17]
T_{16}	The protein p53 binds to p36.	binding	$n_1 * n_6 * 0.01$	[17]
T_{17}	Complex CDK7_cycH binds to complex p36_p53.	binding	$n_7 * n_9 * 0.01$	[17]
T_{18}	Complex CDK7_cycH_p36 phosphorylates the protein p53.	phosphorylation	$n_8 * 0.1$	[17]
T_{19}	The phosphorylated p53 efficiently activates the transcription of the gene <i>p21</i> .	transcription	$n_2 * 0.2$	[17]
T_{20}	Complex p36_p53 activates the transcription of the gene <i>p21</i> .	transcription	$n_9 * 0.1$	[17]
T_{21}	The protein p53 activates the transcription of the gene <i>p21</i> .	transcription	$n_1 * 0.1$	[17]
T_{22}	Translation of <i>p21</i> mRNA.	translation	$n_{10} * 0.1$	[17]

† Corresponding transitions in the HFPN model (Fig. 2). ‡ Speeds of transitions in the HFPN model (Fig. 2). $n_X (X = 1, \dots, 19)$ is the concentration of the corresponding substances in Table 1.

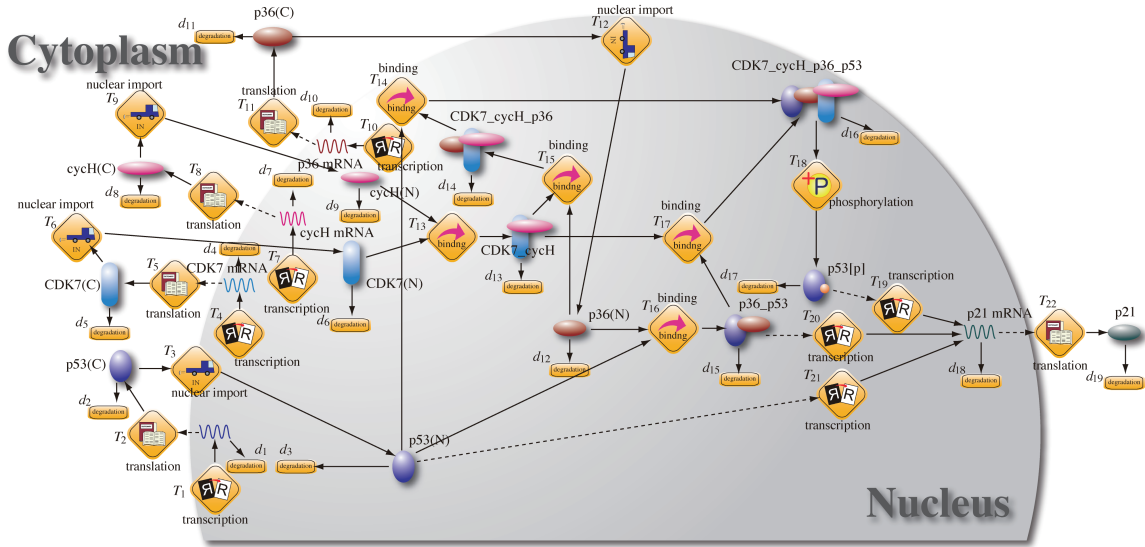


Figure 2: CDK-dependent phosphorylation pathway with hybrid functional Petri net. The pathway represents the complex CDK7_cycH_p36 binds and phosphorylates the protein p53. The phosphorylated protein p53 has the enhanced transcriptional activity which is assigned by the speed of the transitions.

4 Combined Pathway Model and Simulation

We have conducted the protein interactions of p53, MDM2, and p19ARF as the ARF-dependent stabilization pathway for the validation of p53 transcriptional activity with hybrid functional Petri net [11]. CDK-dependent phosphorylation pathway was combined to ARF-dependent stabilization pathway. For the incorporation of quantitative and qualitative alteration of the protein p53, we combine the ARF-dependent stabilization pathway and CDK-dependent phosphorylation pathway.

Fig. 4 shows the combined pathway model which includes whole ARF-dependent stabilization pathway (surrounded with a line) and CDK-dependent phosphorylation pathway (Fig. 2). We add three transitions for the transcriptional activity of phosphorylated p53 and complex p53_MDM2_p19ARF. The transitions T_{23} and T_{24} mean the transcriptional activity of phosphorylated p53 ($p53\{p\}$) for genes *MDM2* and *Bax*, respectively. The transition T_{25} represents the transcriptional activity of complex p53_MDM2_p19ARF that was suggested by our simulation-based validation [11]. The speeds of transitions T_{23} and T_{24} are the same speed of the transition T_{19} , as well as the speed of T_{25} is equal to T_{19} (T_{20}) in the model of [11] (Table. 3).

Fig. 5 is the simulation results of concentration behaviors of p53(N), p36_p53, p53{p}, CDK7(N), p36(N), CDK7_cycH_p36, and p21 mRNA on combinations of p19ARF, CDK7, and p36 expressions. We considered the following cases:

1. All genes including genes *p19ARF*, *CDK7*, and *p36* are expressed.
2. Only the transcription of the gene *p19ARF* is prohibited (remove the transition for the transcription of *p19ARF*).
3. The transcriptions of genes *p19ARF* and *CDK7* are prohibited (remove the transition for the transcription of *p19ARF* and the transition T_4).
4. The transcriptions of three genes ARF, CDK7, and p36 are prohibited (remove the transition for the transcription of *p19ARF*, the transition T_4 , and T_{10}).

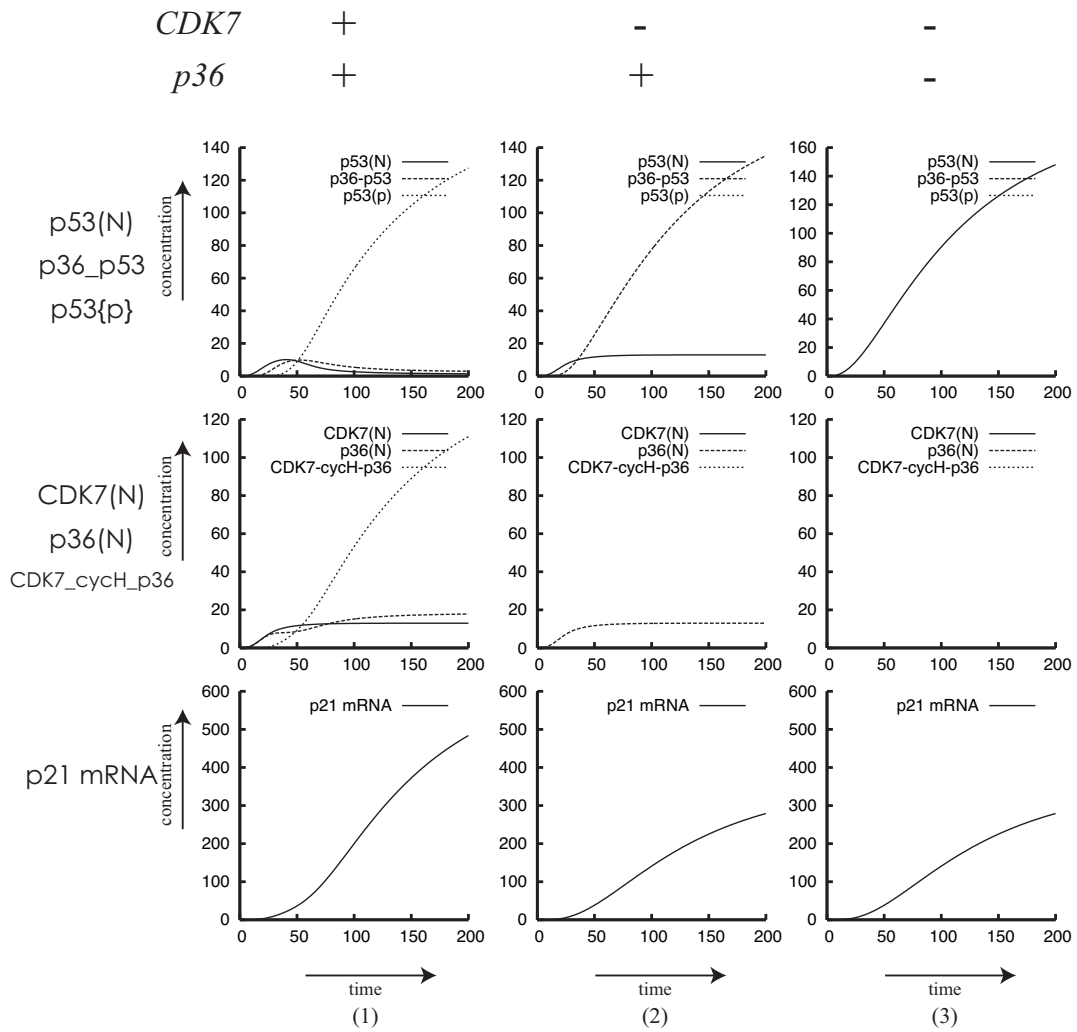


Figure 3: The simulation results of concentration behaviors of p53(N), p36_p53, p53{p}, CDK7(N), p36(N), CDK7_cycH_p36 and p21 mRNA in Fig. 2. +; transactivate the expression of the corresponding genes, -; prohibit the expression of the corresponding genes.

When all genes are expressed, the concentration of p21 mRNA increases by phosphorylated p53 (p53{p}) and complex p53_MDM2_p19ARF. After reaching the peak, it slightly decreases by MDM2 that ubiquitinates the protein p53. When the transcription of the gene *p19ARF* is prohibited, the concentration of p21 mRNA increases by phosphorylated p53 (p53{p}). As well as the case 1, the concentration of p21 mRNA slightly decreases by MDM2 that ubiquitinates the protein p53. When the transcriptions of genes *p19ARF* and *CDK7* are prohibited, the concentration of p21 mRNA increases by complex p36_p53, and slightly decreases by MDM2 that ubiquitinates the protein p53. When the transcriptions of three genes *p19ARF*, *CDK7*, and *p36* are prohibited, the concentration of p21 mRNA do not increase. From Fig. 5 (1) and 5 (2), we observed the effect of ARF-dependent stabilization pathway. In spite of the destabilization of p53(N), phosphorylated p53 still have a efficient transcriptional activity (Fig. 5 (2)). Comparing Fig. 5 (2) and 5(3), we could not observed the obvious difference in the amount of p21 mRNA.

Table 3: The transitions T_{23} , T_{24} , and T_{25} are for the combined pathway (Fig. 4).

T_i^\dagger	biological phenomena on the literature	type of biological processes	\ddagger	literature
T_{23}	The phosphorylated p53 activates the transcription of the gene <i>p21</i> .	transcription	$n2 * 0.2$	–
T_{24}	The phosphorylated p53 activates the transcription of the gene <i>p21</i> .	transcription	$n2 * 0.2$	–
T_{25}	The complex p53_MDM2_p19ARF activates the transcription of the gene <i>p21</i> .	transcription	$m3 * 0.1$	–

\dagger Corresponding transitions in the HFPN model (Fig. 4). \ddagger Speeds of transitions in the HFPN model (Fig. 4). $n2$ is the concentration of phosphorylated p53 (p53{p}). $m3$ is the concentration of complex p53_MDM2_p19ARF [11].

5 Discussion and Conclusion

Through the simulations (Fig. 3 and Fig. 5), we observed the effects of CDK-dependent phosphorylation and ARF-dependent stabilization. Since phosphorylated protein p53 has a enhanced transcriptional activity for p21 mRNA, CDK-dependent phosphorylation pathway provides the results that the lack of CDK decreases the concentration of p21 mRNA, comparing Fig. 3 (1) and Fig. 3 (2). As shown in Fig. 5 (2) and Fig. 5(3), contrary to expectation, the lack of CDK7 seemed to have no effect to the concentration of p21 mRNA. In addition to the concentration of p21 mRNA, the phosphorylated protein p53 (p53{p}) increases the concentration of MDM2 mRNA (Fig. 4). While the protein p53 is phosphorylated, the protein MDM2 decreases the concentration of the protein p53 more effectively. Although the complex p36_p53 has a lessor transcriptional activity than that of p53{p}, the concentration of p36_p53 is higher than that of p53{p}. From these fact, the concentration of p21 mRNA was not changed whether or not the transcription of CDK7 was prohibited.

On the assumption that the protein MDM2 could not phosphorylate the complex p36_p53, we combined CDK-dependent phosphorylation pathway and ARF-dependent stabilization pathway. Thereby, the protein p36 performed like the protein p19ARF and stabilized the concentration of the protein p53. Acutually, biologists suggested that the protein MDM2 has a low binding affinity with the phosphorylated protein p53 [24].

We demonstrated the effect which was not observed in the single pathway, combining two pathways. Therefore we have to consider both phosphorylation and stabilization pathway when we investigate the transcription activity of the protein p53. Modeling and simulation of biological pathways saves the costs of biological experiments from both sides of expanse and time. In fact, we could not estimate the

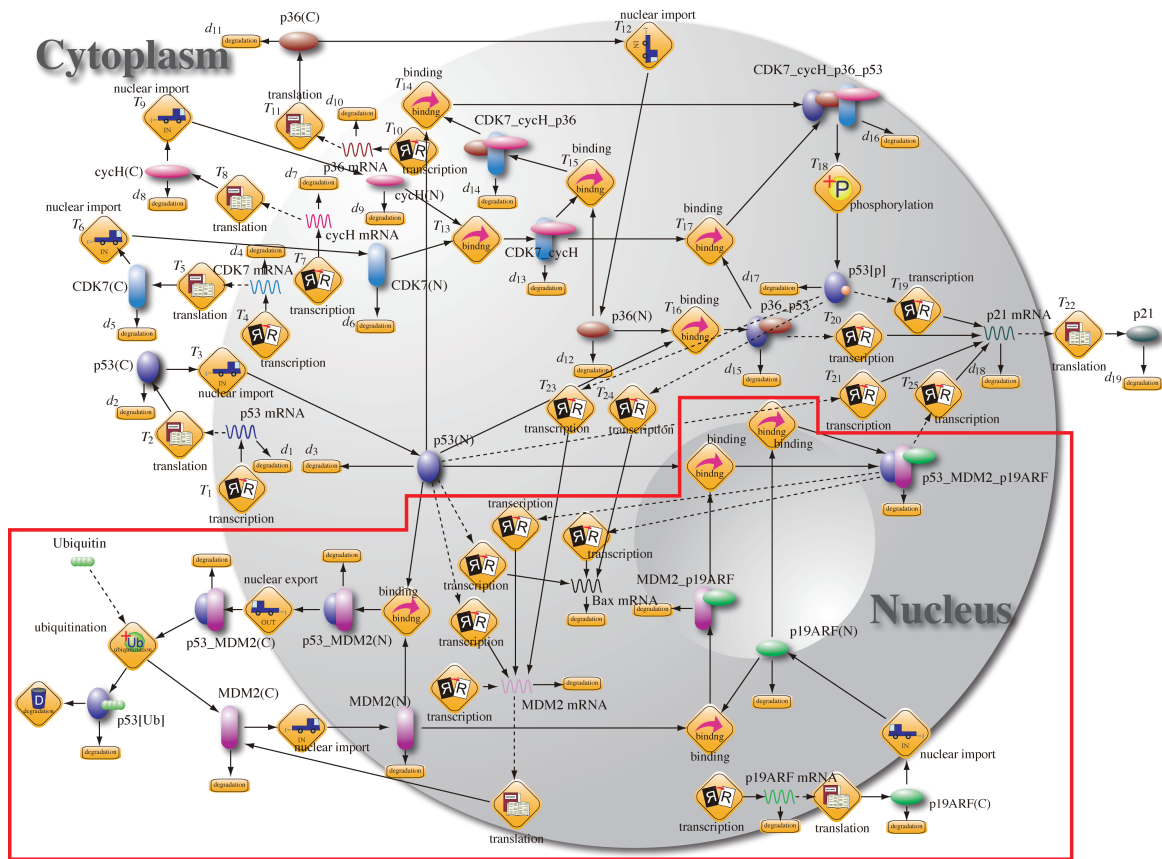


Figure 4: A merged pathway that includes the ARF-dependent stabilization pathway (surrounded with a line) and CDK-dependent phosphorylation pathway (Fig. 2). The transitions T_{23} and T_{24} mean the transcriptional activity of phosphorylated p53 ($p53\{p\}$) for genes *MDM2* and *Bax*, respectively. The transition T_{25} represents the transcriptional activity of complex $p53_MDM2_p19ARF$ that was suggested by our simulation-based validation [11].

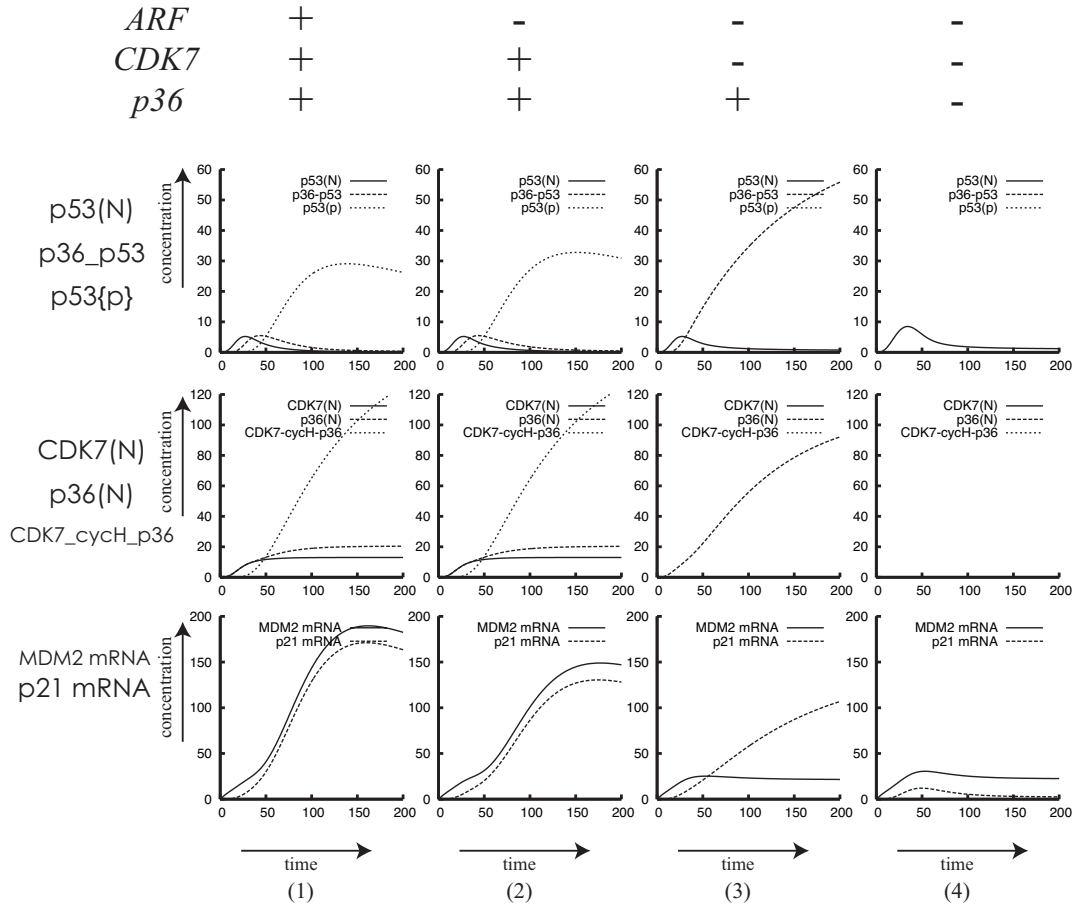


Figure 5: The simulation results of concentration behaviors of p53(N), p36_p53, p53{p}, CDK7(N), p36(N), CDK7_cycH_p36, MDM2 mRNA and p21 mRNA in Fig. 4. +; transactivate the expression of the corresponding genes, -; prohibit the expression of the corresponding genes.

accuracy of the simulation result, since there are considerable differences in the biological experiments such as cell types, tissue types, and experimental protocols. Furthermore, the protein p53 has several phosphorylation sites at the N-terminal and C-terminal regions. A kinase specifically phosphorylates p53 at different positions. Recently, we have developed a new biological pathway description format in XML called Cell System Markup Language (CSML) [5]. By using the CSML, we intend to store the information of phosphorylation sites with pathway models and apply the positional information to the simulation.

References

- [1] <http://biocyc.org/>.
- [2] <http://www.genome.jp/kegg/pathway/hsa/hsa04110.html>.
- [3] <http://www.biobase.de/>.
- [4] http://www.fqspl.com.pl/life_science/cellillustrator/ci.htm.
- [5] <http://www.csml.org/>.
- [6] Alla, H. and David, R. Continuous and hybrid Petri nets. *J. Circuits, Systems, and Computers*, 8(1):159–188, 1998.
- [7] Blaydes, J. P., Luciani, M. G., Pospisilova, S., Ball, H. M., Vojtesek, B., and Hupp, T. R. Stoichiometric phosphorylation of human p53 at ser315 stimulates p53-dependent transcription. *J. Biol. Chem.*, 276(7):4699–4708, 2001.
- [8] Datta, N. S. and Long, M. W. Modulation of mdm2/p53 and cyclin-activating kinase during the megakaryocyte differentiation of human erythroleukemia cells. *Exp. Hematol.*, 30(2):158–165, 2002.
- [9] Doi, A., Fujita, S., Matsuno, H., Nagasaki, M., and Miyano, S. Constructing biological pathway models with hybrid functional Petri net. *In Silico Biol.*, 4(3):271–291, 2004. <<http://www.bioinfo.de/isb/2004/04/0023>>.
- [10] Doi, A., Nagasaki, M., Fujita, S., Matsuno, H., and Miyano, S. Genomic object net: II. modelling biopathways by hybrid functional Petri net with extension. *Appl. Bioinformatics*, 2(3):185–188, 2003.
- [11] Doi, A., Nagasaki, M., Matsuno, H., and Miyano, S. Simulation based validation of the p53 transcriptional activity with hybrid functional Petri net. *In Silico Biol.*, 6(0001), 2006. <<http://www.bioinfo.de/isb/2006/06/0001>>.
- [12] Kamijo, T., Weber, J. D., Zambetti, G., Zindy, F., Roussel, M. F., and Sherr, C. J. Functional and physical interactions of the arf tumor suppressor with p53 and mdm2. *Proc. Natl. Acad. Sci. USA*, 95(14):8292–8297, 1998.
- [13] Kanehisa, M. and Goto, S. KEGG: kyoto encyclopedia of genes and genomes. *Nucleic Acids Res.*, 28(1):27–30, 2000.
- [14] Ko, L. J., Shieh, S. Y., Chen, X., Jayaraman, L., Tamai, K., Taya, Y., Prives, C., and Pan, Z. Q. p53 is phosphorylated by cdk7-cyclin h in a p36mat1-dependent manner. *Mol. Cell. Biol.*, 17(12):7220–7229, 1997.

- [15] Krull, M., Voss, N., Choi, C., Pistor, S., Potapov, A., and E., W. TRANSPATH: an integrated database on signal transduction and a tool for array analysis. *Nucleic Acids Res.*, 31(1):97–100, 2003.
- [16] Liu, L., Scolnick, D. M., Trievel, R. C., Zhang, H. B., Marmorstein, R., Halazonetis, T. D., and Berger, S. L. p53 sites acetylated in vitro by pcaf and p300 are acetylated in vivo in response to dna damage. *Mol. Cell. Biol.*, 19(2):1202–1209, 1999.
- [17] Lu, H., Fisher, R. P., Bailey, P., and Levine, A. J. The cdk7-cych-p36 complex of transcription factor ihh phosphorylates p53, enhancing its sequence-specific dna binding activity in vitro. *Mol. Cell. Biol.*, 17(10):5923–5934, 1997.
- [18] Matsuno, H., Doi, A., Hirata, Y., and Miyano, S. XML documentation of biopathways and their simulations in Genomic Object Net. *Genome Inform.*, 12:54–62, 2001.
- [19] Matsuno, H., Doi, A., Nagasaki, M., and Miyano, S. Hybrid Petri net representation of gene regulatory network. *Pac. Symp. Biocomput.*, 5:341–352, 2000.
- [20] Matsuno, H., Tanaka, Y., Aoshima, H., Doi, A., Matsui, M., and Miyano, S. Biopathways representation and simulation on hybrid functional petri net. *In Silico Biol.*, 3(3):389–404, 2003. <http://www.bioinfo.de/isb/toc_vol_03.html>.
- [21] Nagasaki, M., Doi, A., Matsuno, H., and Miyano, S. Genomic object net: I. a platform for modeling and simulating biopathways. *Appl. Bioinformatics*, 2(3):181–184, 2003.
- [22] Pomerantz, J., Schreiber-Agus, N., Liegeois, N. J., Silverman, A., Alland, L., Chin, L., Potes, J., Chen, K., Orlow, I., Lee, H. W., Cordon-Cardo, C., and DePinho, R. A. The Ink4a tumor suppressor gene product p19Arf interacts with MDM2 and neutralizes MDM2's inhibition of p53. *Cell*, 92(6):713–723, 1998.
- [23] Reisig, W. *Petri Nets*. Springer-Verlag, Berlin, 1985.
- [24] Sakaguchi, K., Saito, S., Higashimoto, Y., Roy, S., Anderson, C., and Appella, E. Damage-mediated phosphorylation of human p53 threonine 18 through a cascade mediated by a casein 1-like kinase. effect on mdm2 binding. *J. Biol. Chem.*, 275(13):9278–9283, 2000.
- [25] Taylor, S. L., Kinchington, P. R., Brooks, A., and Moffat, J. F. Roscovitine, a cyclin-dependent kinase inhibitor, prevents replication of varicella-zoster virus. *J. Virol*, 78(6):2853–2862, 2004.
- [26] Xie, S., Wang, Q., Wu, H., Cogswell, J., Lu, L., Jhanwar-Uniyal, M., and Dai, W. Reactive oxygen species-induced phosphorylation of p53 on serine 20 is mediated in part by polo-like kinase-3. *J. Biol. Chem.*, 276(39):36194–36199, 2001.
- [27] Xie, S., Wu, H., Wang, Q., Cogswell, J. P., Husain, I., Conn, C., Stambrook, P., Jhanwar-Uniyal, M., and Dai, W. Plk3 functionally links dna damage to cell cycle arrest and apoptosis at least in part via the p53 pathway. *J. Biol. Chem.*, 276(46):43305–43312, 2001.
- [28] Zhang, Y., Xiong, Y., and Yarbrough, W. G. Arf promotes mdm2 degradation and stabilizes p53: Arf-ink4a locus deletion impairs both the rb and p53 tumor suppression pathways. *Cell*, 92(6):725–734, 1998.